Supplementary information

"A compact micro-load compression testing device for stiffness characterization of soft biological samples" by Nakao *et al*.

Supplementary Table 1. Conditions for milling the indenter and saucer.

		Indenter	Bowl-shaped saucer		Flat saucer	
			Top	Bottom	Top	Bottom
Bulk material		POM	POM		POM	
Roughing process	Cutting tool (end mill)	Square	Square	Square	Square	Square
	Blade diameter [mm]	1.0	1.0	1.0	1.0	1.0
	Spindle revolution [rpm]	7,000	7,000	7,000	7,000	7,000
	Cutting speed [mm/min]	600	600	600	600	600
	Depth of cut [μm]	100	100	100	100	100
	Path interval [μm]	100	100	100	100	100
	Machining allowance [μm]	200	200	200	200	200
Finishing process	Cutting tool (end mill)	Square	Ball	Square	Square	Square
	Blade diameter [mm]	1.0	R0.5	1.0	1.0	1.0
	Spindle revolution [rpm]	7,000	7,000	7,000	7,000	7,000
	Cutting speed [mm/min]	600	600	600	600	600
	Depth of cut [μm]	50	100	50	50	50
	Path interval [μm]	50	100	50	50	50
	Machining allowance [μm]	0	0	0	0	0

Supplementary Table 2. Conditions for milling the sample molds.

		Sphere (Collagen)	Sphere (Gelatin)	Cylinder (Gelatin)	
				Frame	Base
Bulk material		BNF-PMSQ	PTFE	PTFE	
Roughing process	Cutting tool (end mill)	Ball	Square	Square	Square
	Blade diameter [mm]	R0.4	0.4	3.0	3.0
	Spindle revolution [rpm]	7,000	7,000	7,000	7,000
	Cutting speed [mm/min]	960	600	1,000	1,000
	Depth of cut [μm]	100	50	200	200
	Path interval [μm]	100	50	500	500
	Machining allowance [μm]	100	100	300	300
Finishing process	Cutting tool (end mill)	Ball	Ball	Square	Square
	Blade diameter [mm]	R0.4	R0.4	3.0	3.0
	Spindle revolution [rpm]	7,000	7,000	7,000	7,000
	Cutting speed [mm/min]	1,000	600	800	800
	Depth of cut [μm]	100	10	100	100
	Path interval [μm]	100	10	100	100
	Machining allowance [μm]	0	0	0	0

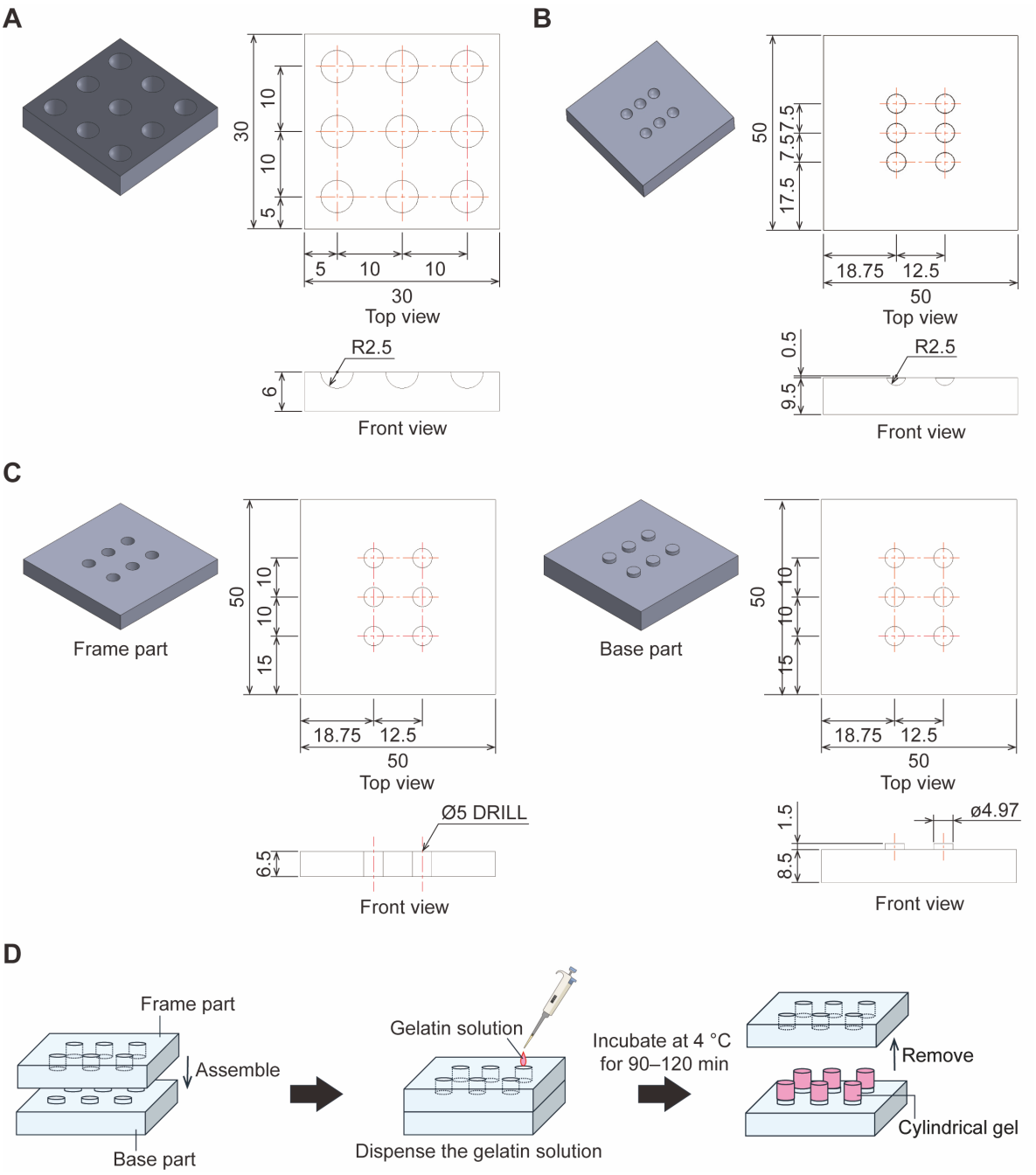

Supplementary Fig. 1. Dimensions and configurations of molds used for sample fabrication. (**A**) Mold for spherical collagen samples machined from a superhydrophobic material (BNF-PMSQ). (**B**) Mold for spherical gelatin samples machined from PTFE. (**C**) Mold for cylindrical gelatin samples machined from PTFE, consisting of frame and base parts. All dimensional values shown in (**A**–**C**) are given in millimeters (mm). (**D**) Schematic illustration showing the assembly and usage of the mold for cylindrical sample fabrication.

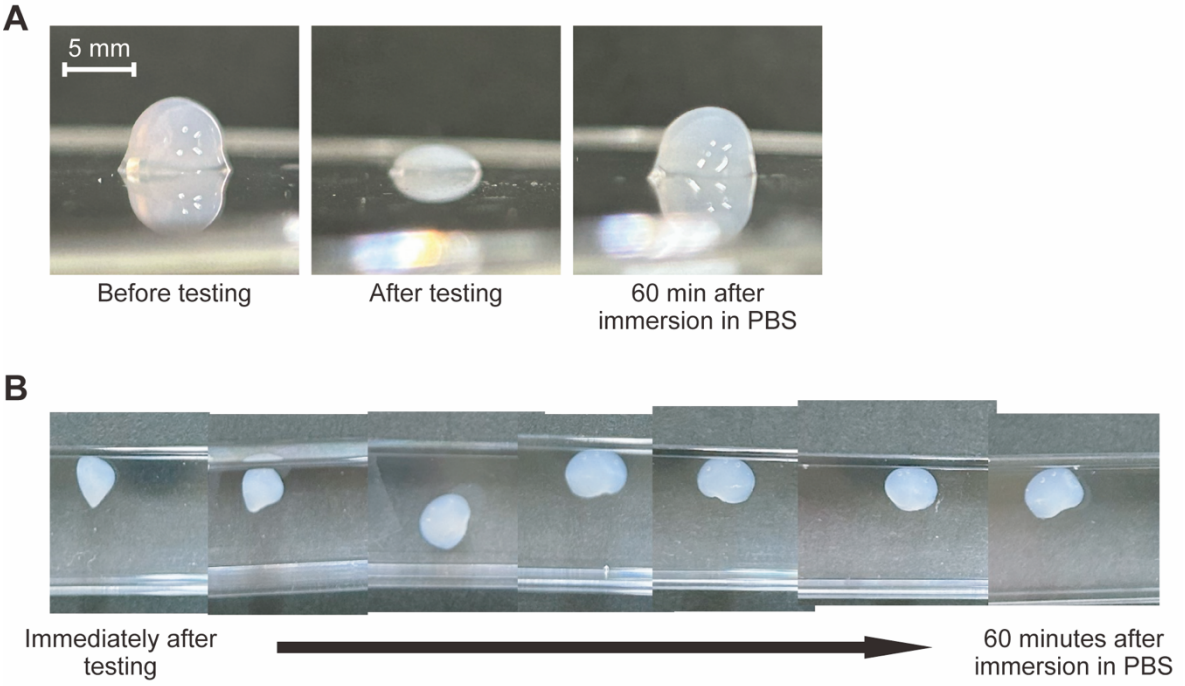

Supplementary Fig. 2. Shape recovery of spherical collagen samples after compression testing at 18 °C. (**A**) Photographs of a spherical collagen sample before compression testing, immediately after testing, and after 60 min of immersion in PBS. The sample partially recovers its original shape upon re-immersion in PBS. (**B**) Time-lapse photographs showing the shape recovery of the collagen sample during immersion in PBS, acquired at 10-min intervals from immediately after testing to 60 min after immersion. PBS has a near-isotonic osmolarity to the surrounding media (DMEM), constituting the collagen sample, thereby minimizing osmotic effects during immersion.

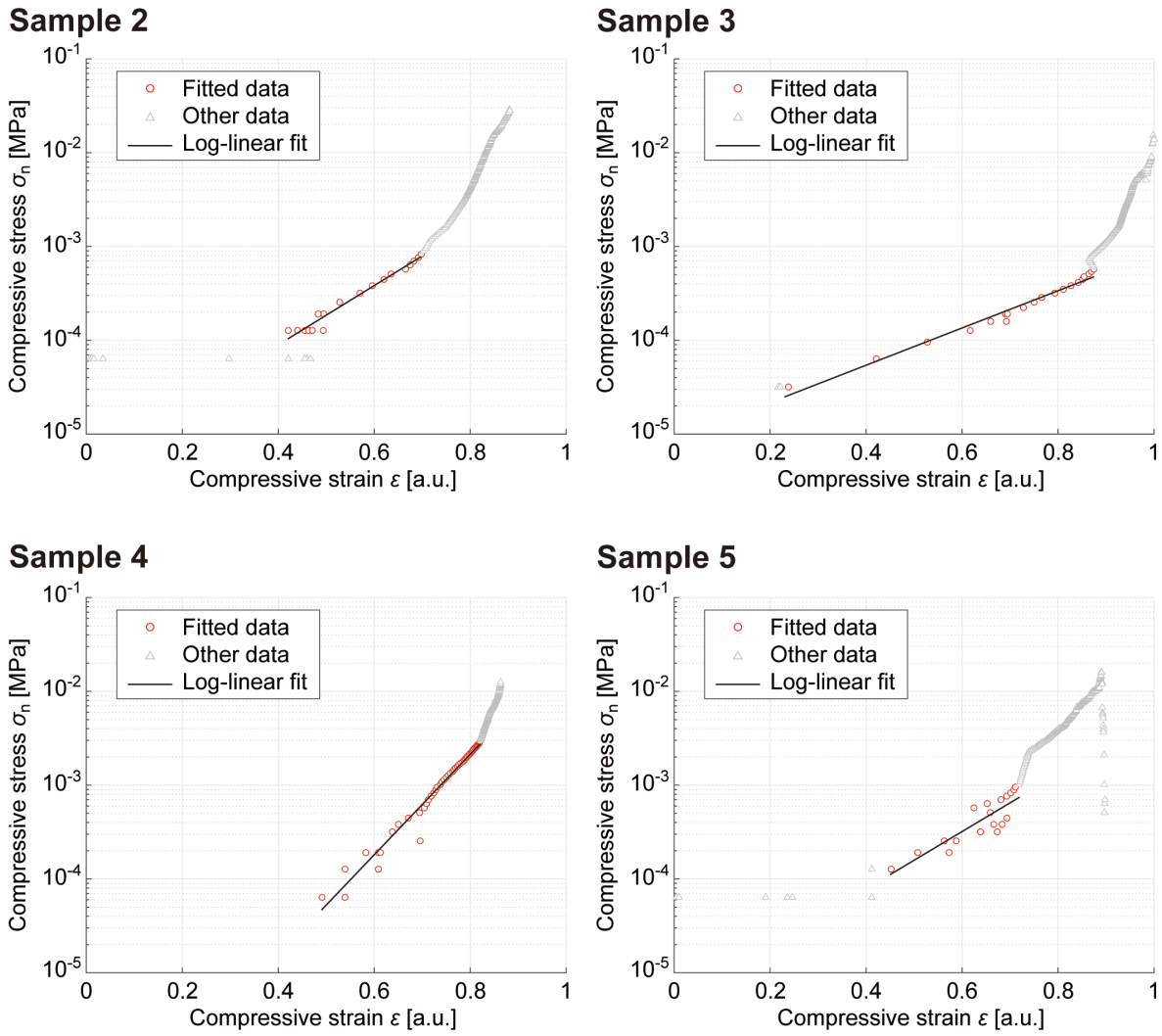

Supplementary Fig. 3. Reproducibility of compressive behavior in spherical collagen samples at 18 °C. Stress–strain curves obtained from independent measurements of spherical collagen samples at 18 °C, corresponding to samples 2–5. The data demonstrate the reproducibility of the compressive response shown in **Fig. 3A**.

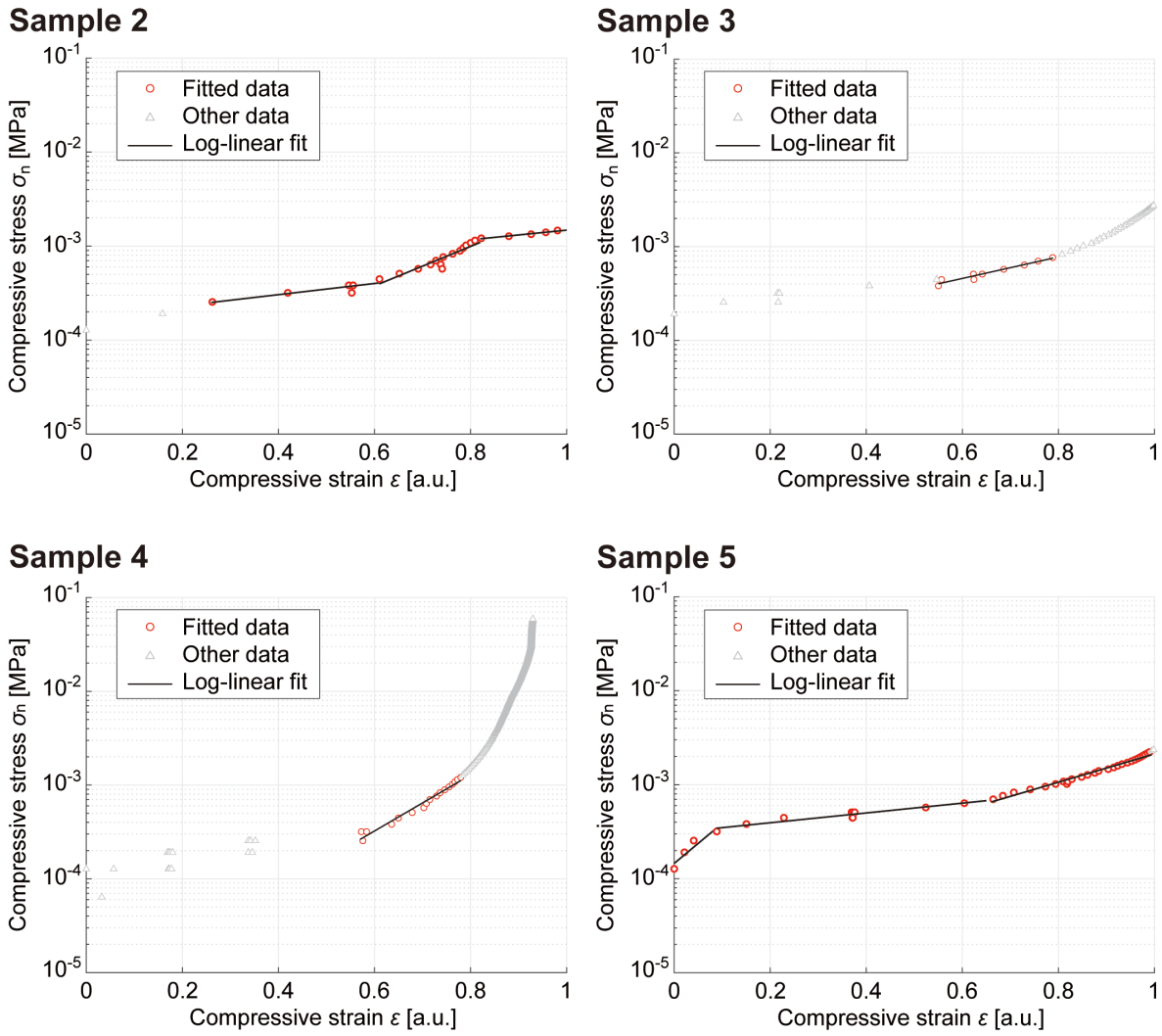

Supplementary Fig. 4. Reproducibility of compressive behavior in spherical collagen samples at 5 °C. Stress–strain curves obtained from independent measurements of spherical collagen samples at 5 °C, corresponding to samples 2–5. The data demonstrate the reproducibility of the compressive response shown in **Fig. 3B**. For samples in which fitting was performed in three distinct regions (samples 2 and 5), the second fitting region was selected for analysis, as it corresponded to the linear strain region used for comparison in the other samples.

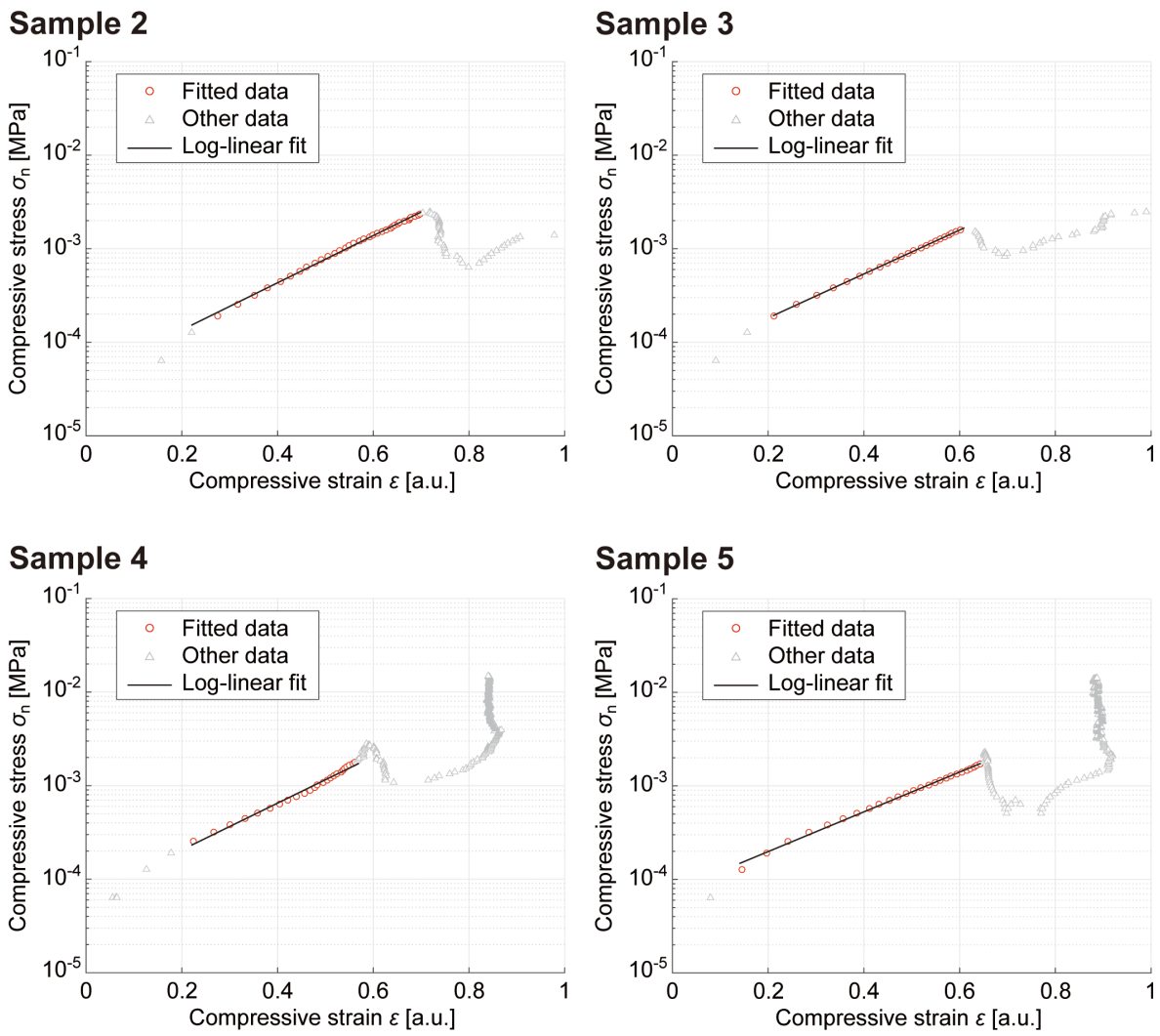

Supplementary Fig. 5. Reproducibility of compressive behavior in spherical gelatin samples at 18 °C. Stress–strain curves obtained from independent measurements of spherical gelatin samples at 18 °C, corresponding to samples 2–5. The data demonstrate the reproducibility of the compressive response shown in **Fig. 4A**.

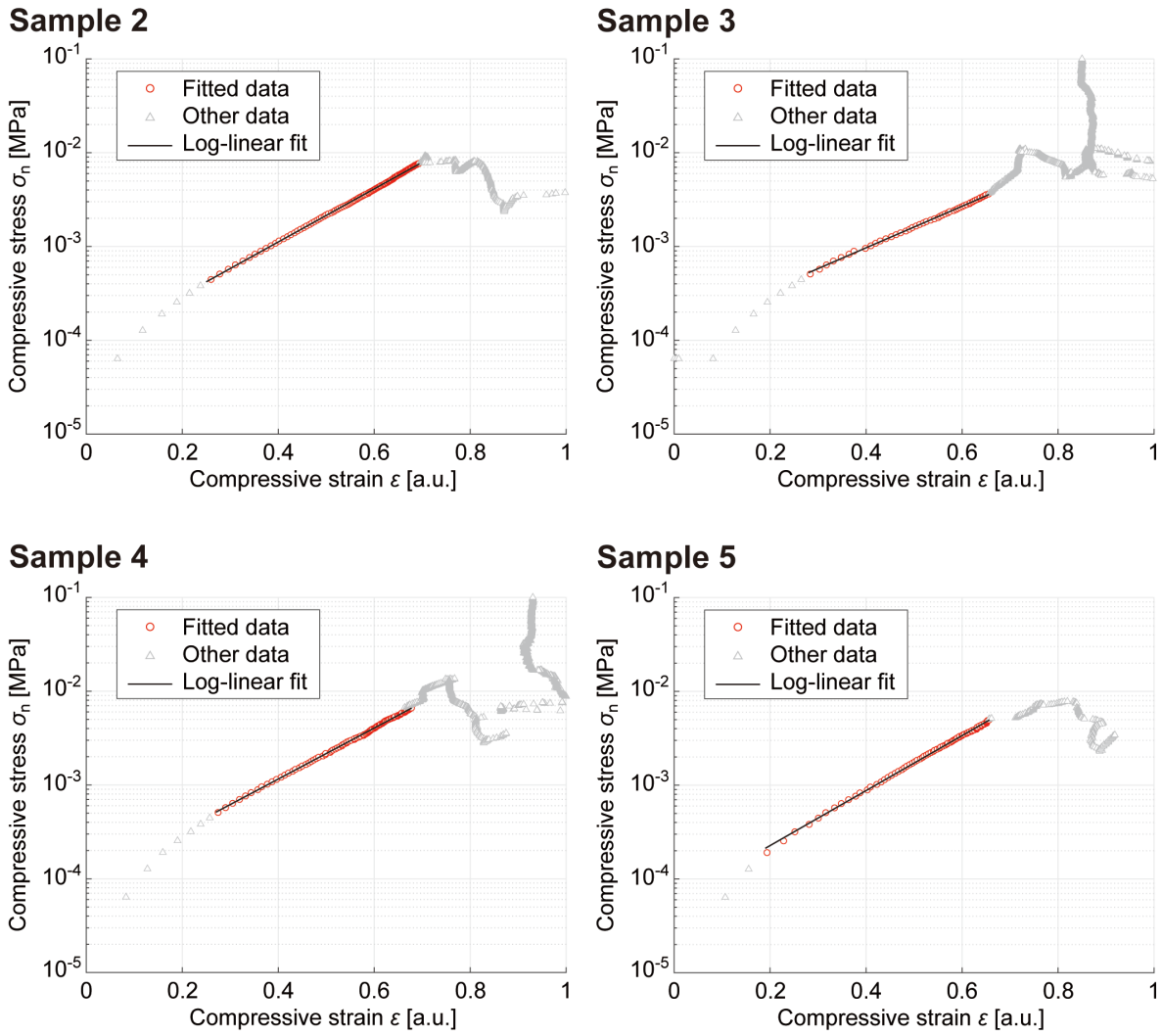

Supplementary Fig. 6. Reproducibility of compressive behavior in spherical gelatin samples at 5 °C. Stress–strain curves obtained from independent measurements of spherical gelatin samples at 5 °C, corresponding to samples 2–5. The data demonstrate the reproducibility of the compressive response shown in **Fig. 4B**.

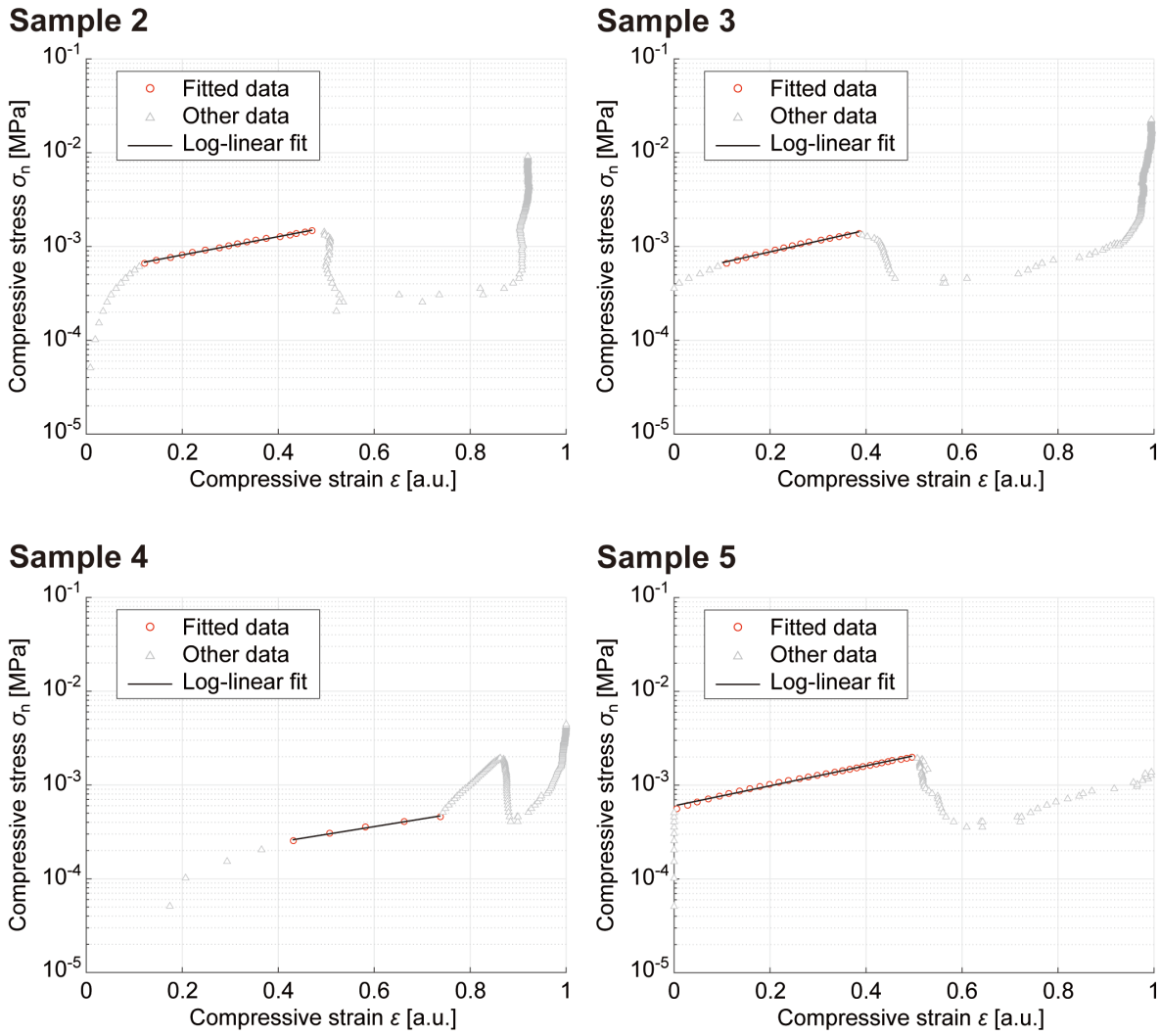

Supplementary Fig. 7. Reproducibility of compressive behavior in cylindrical gelatin samples at 18 °C. Stress–strain curves obtained from independent measurements of cylindrical gelatin samples at 18 °C, corresponding to samples 2–5. The data demonstrate the reproducibility of the compressive response shown in **Fig. 4C**.

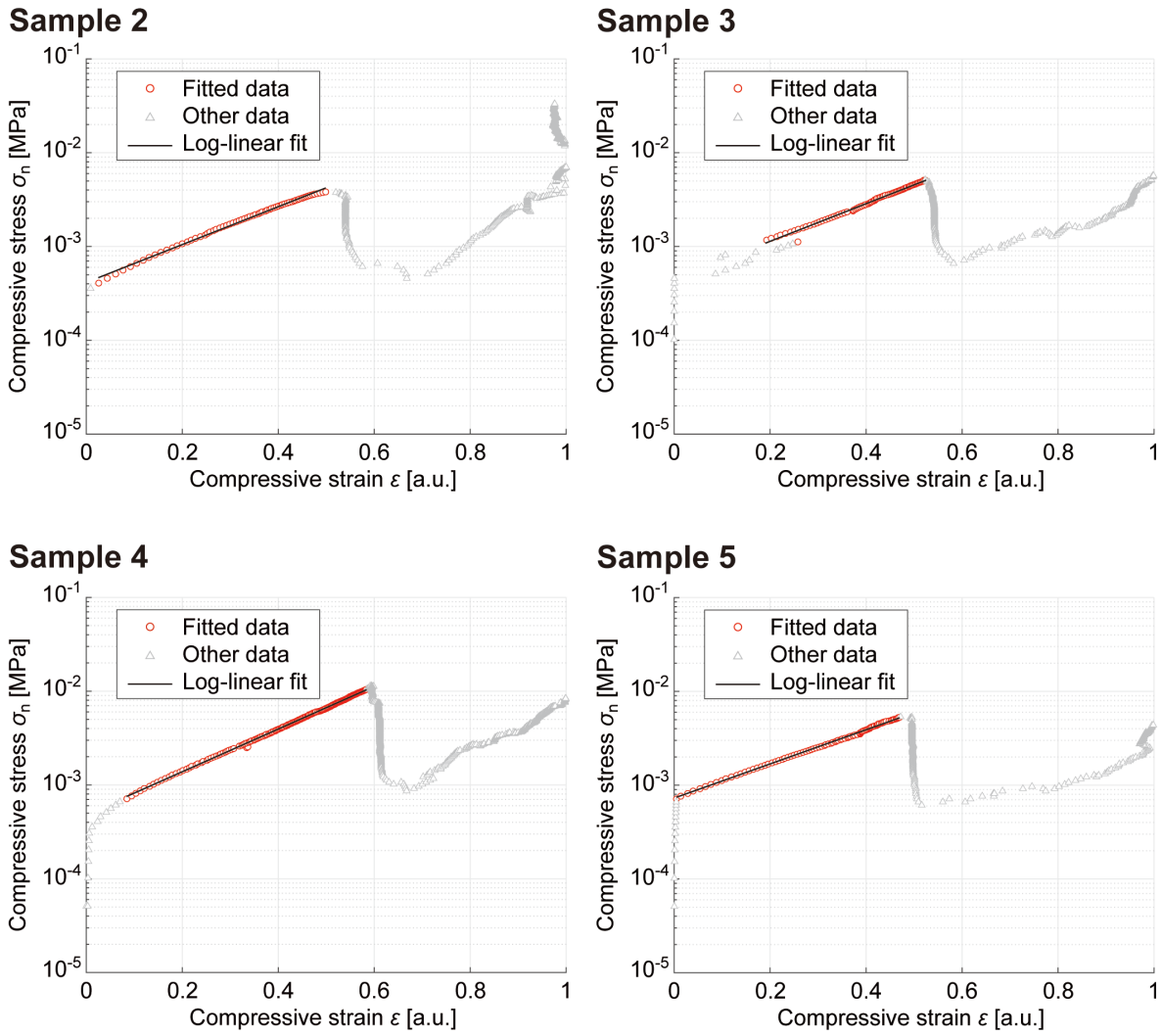

Supplementary Fig. 8. Reproducibility of compressive behavior in cylindrical gelatin samples at 5 °C. Stress–strain curves obtained from independent measurements of cylindrical gelatin samples at 5 °C, corresponding to samples 2–5. The data demonstrate the reproducibility of the compressive response shown in **Fig. 4D**.

Sample 1 (Fig. 3A)

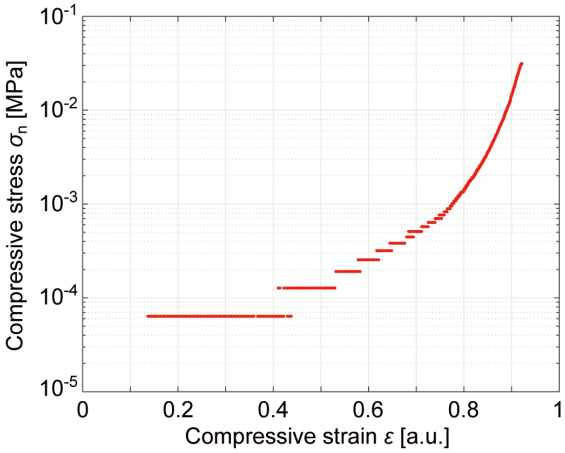

Sample 2

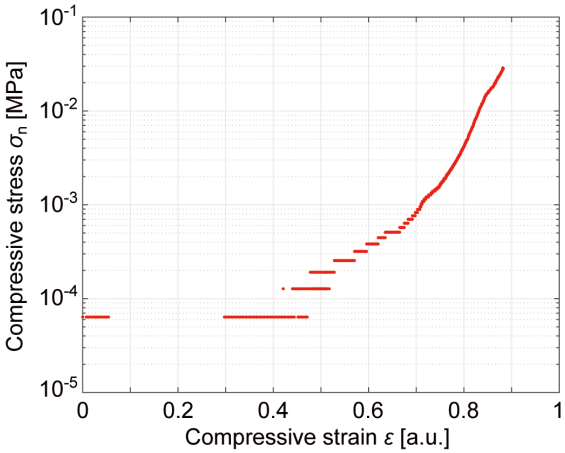

Sample 3

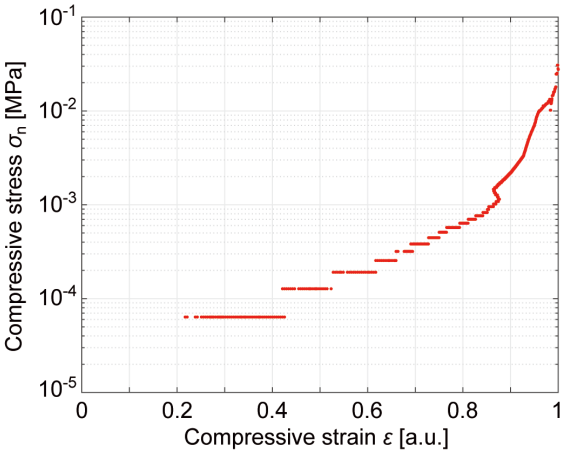

Sample 4

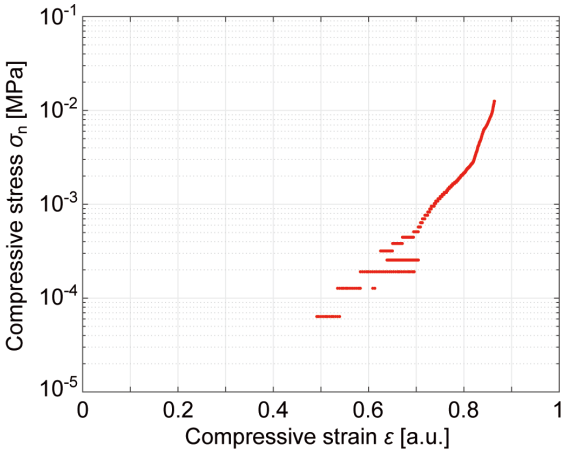

Sample 5

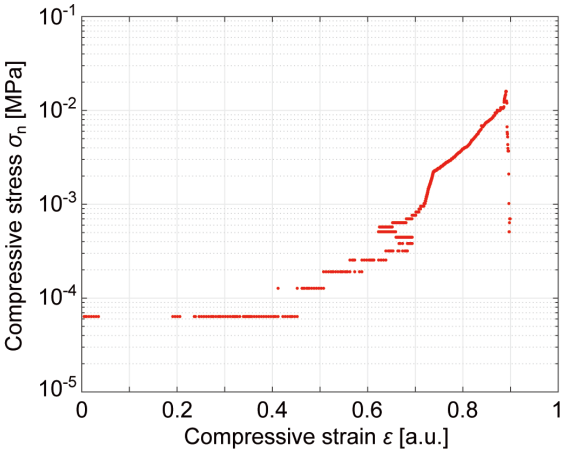

Supplementary Fig. 9. Raw stress–strain data for spherical collagen samples at 18 °C.

Sample 1 (Fig. 3B)

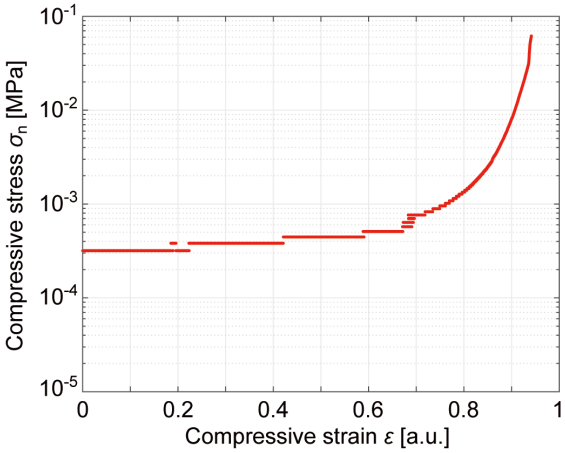

Sample 2

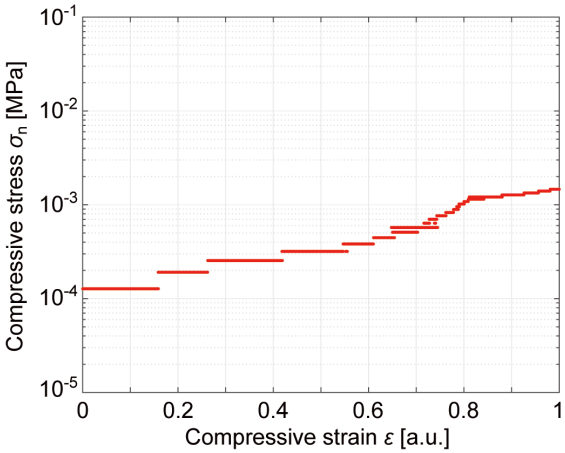

Sample 3

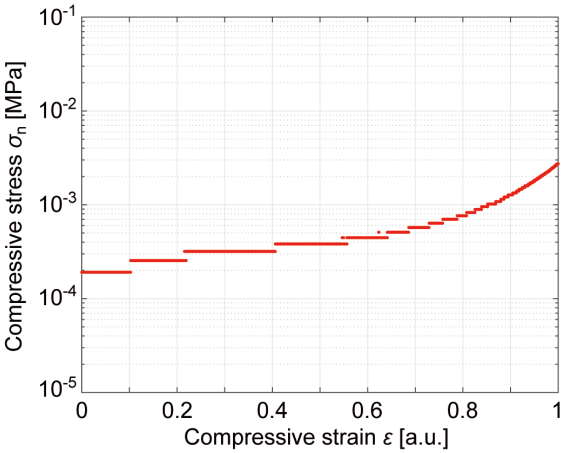

Sample 4

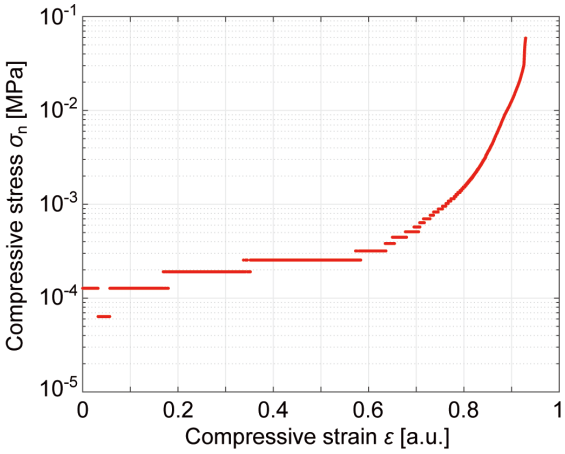

Sample 5

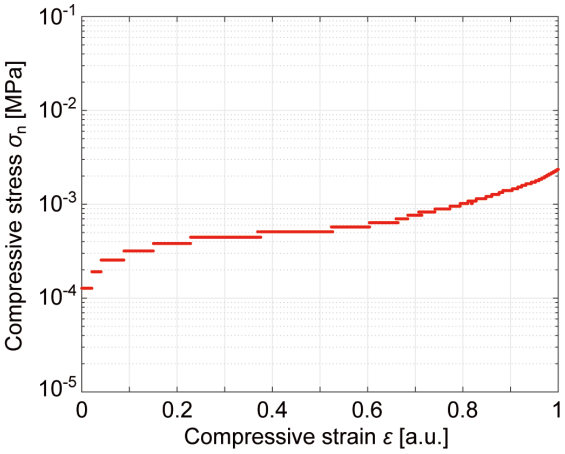

Supplementary Fig. 10. Raw stress–strain data for spherical collagen samples at 5 °C.

Sample 1 (Fig. 4A)

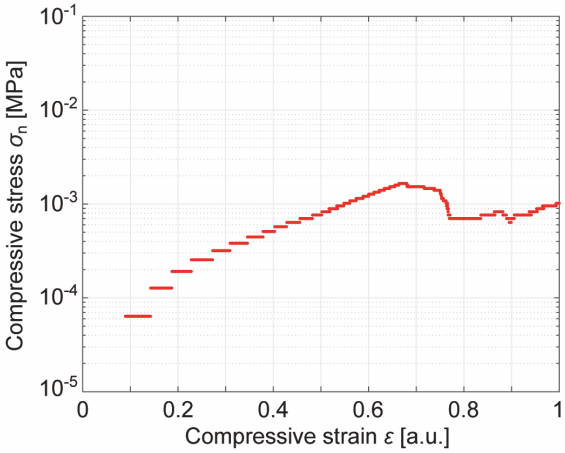

Sample 2

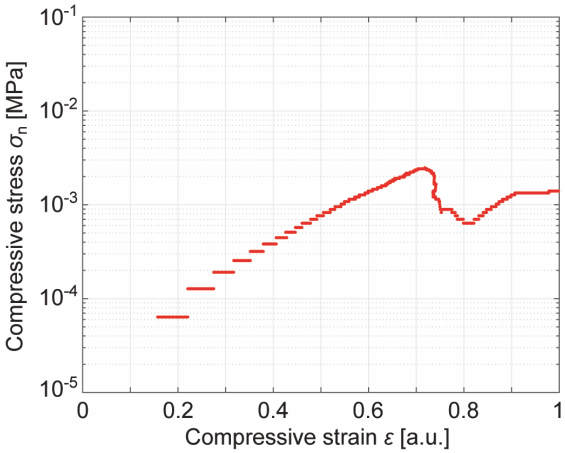

Sample 3

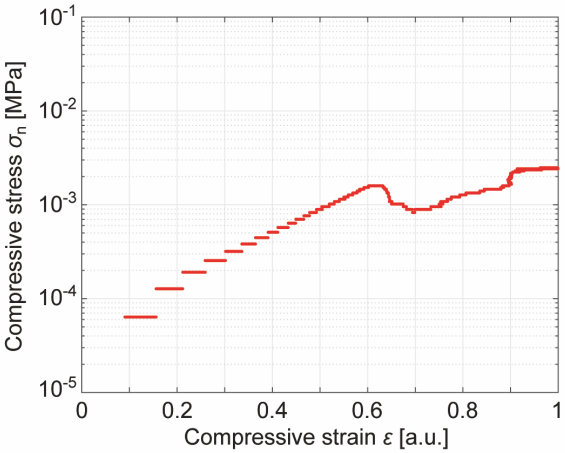

Sample 4

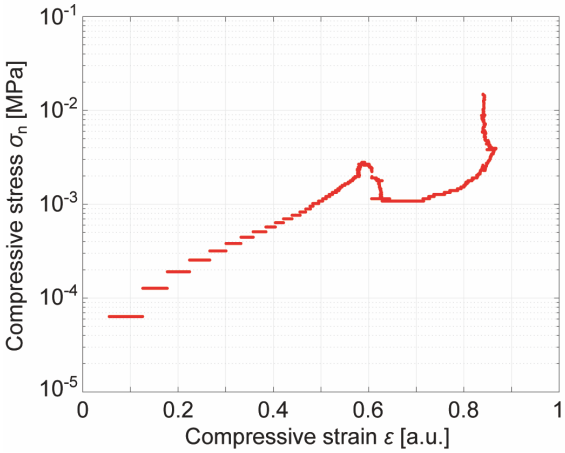

Sample 5

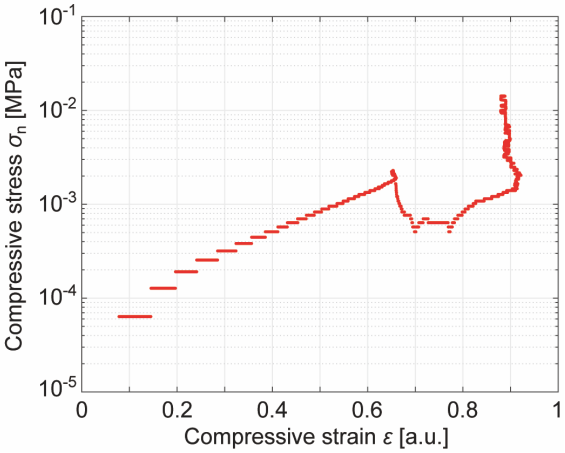

Supplementary Fig. 11. Raw stress–strain data for spherical gelatin samples at 18 °C.

Sample 1 (Fig. 4B)

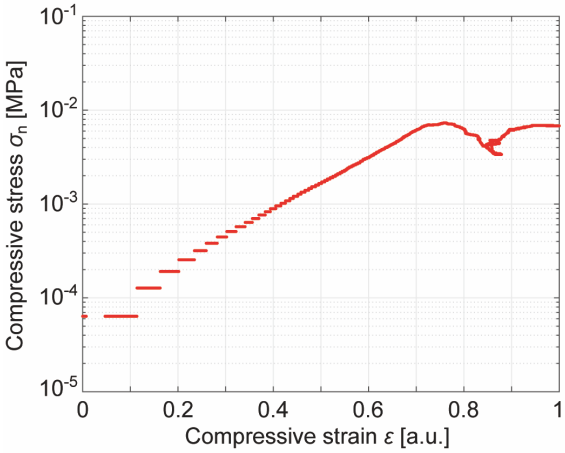

Sample 2

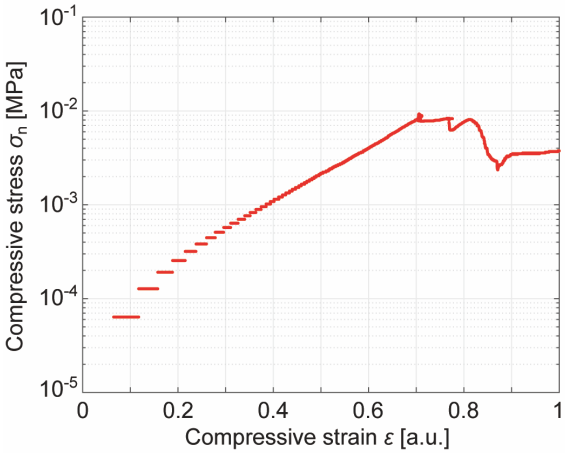

Sample 3

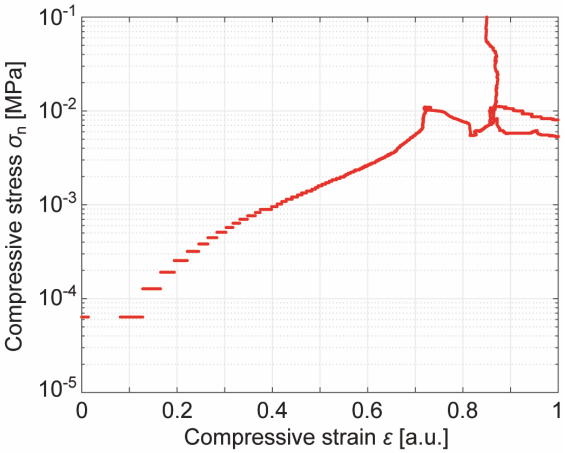

Sample 4

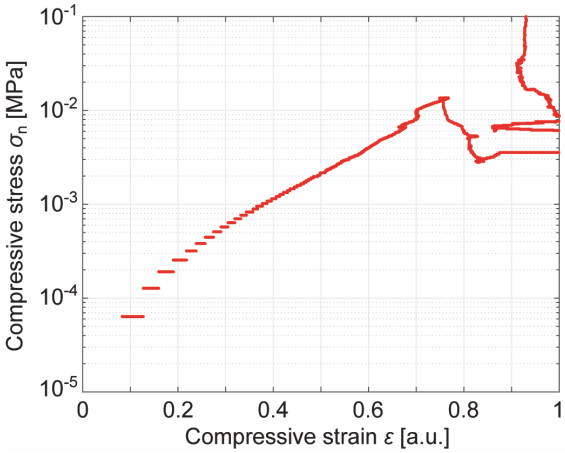

Sample 5

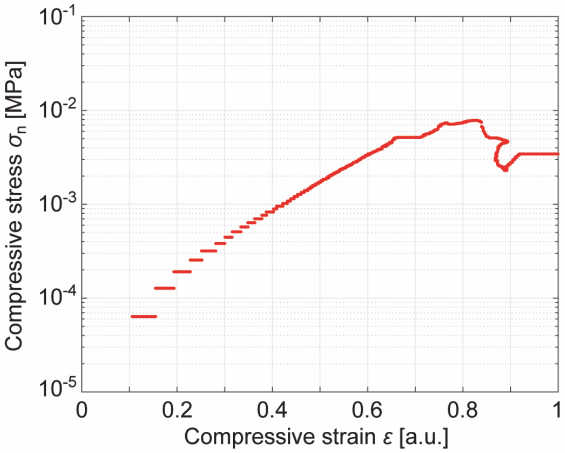

Supplementary Fig. 12. Raw stress–strain data for spherical gelatin samples at 5 °C.

Sample 1 (Fig. 4C)

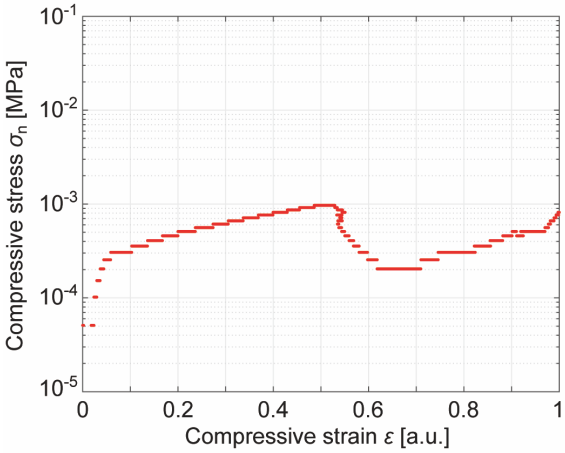

Sample 2

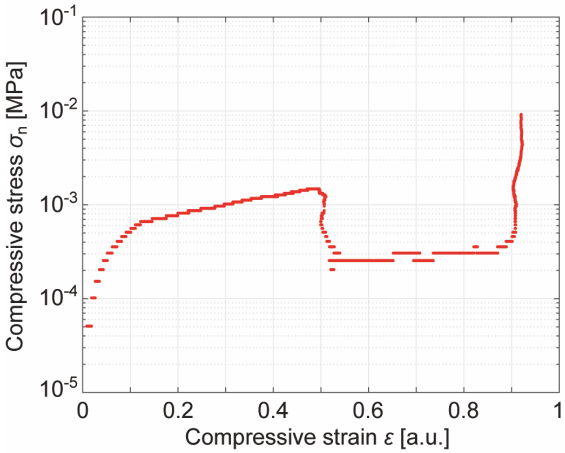

Sample 3

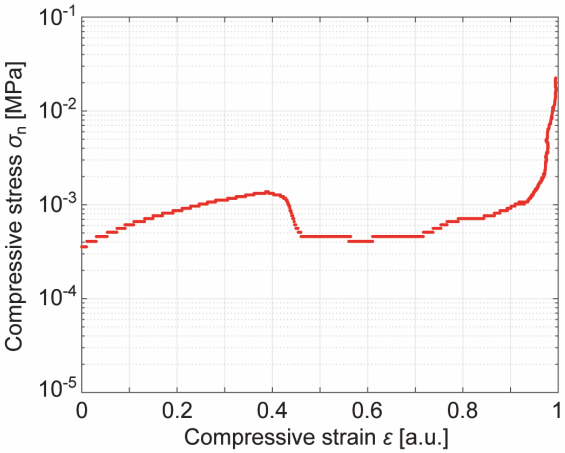

Sample 4

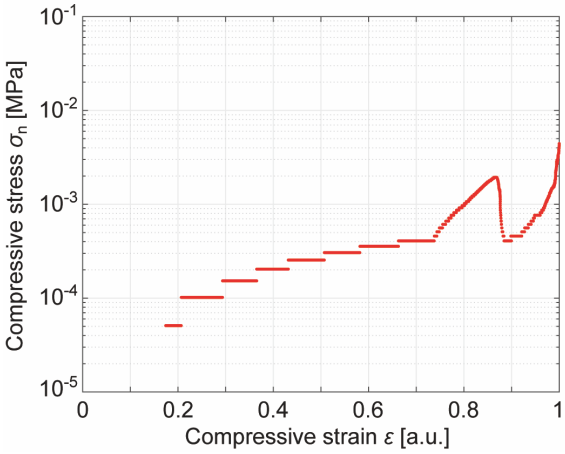

Sample 5

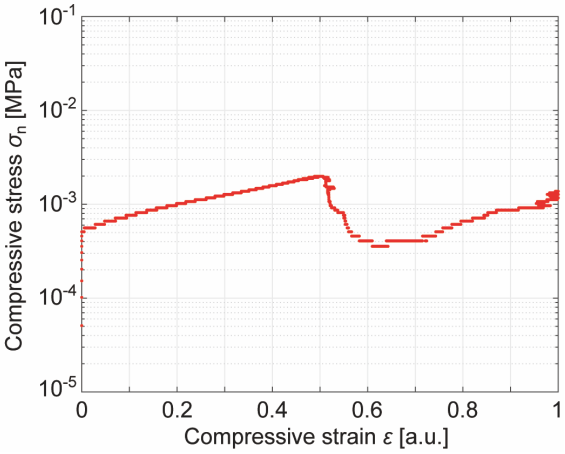

Supplementary Fig.13. Raw stress–strain data for cylindrical gelatin samples at 18 °C.

Sample 1 (Fig. 4D)

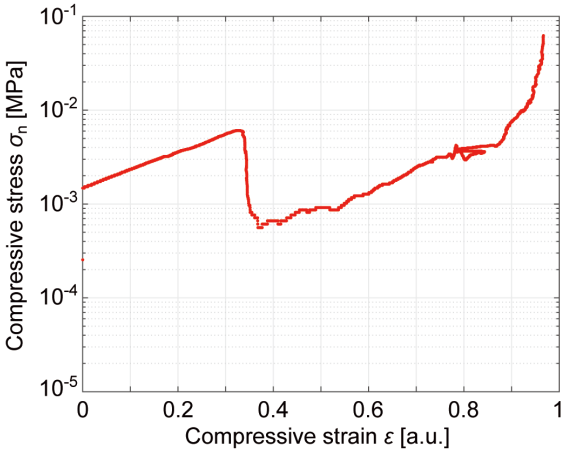

Sample 2

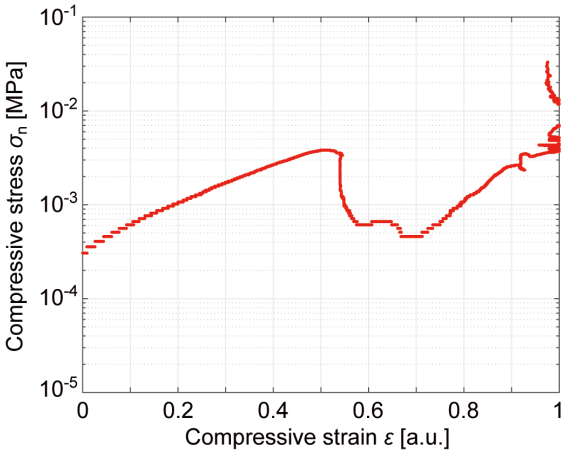

Sample 3

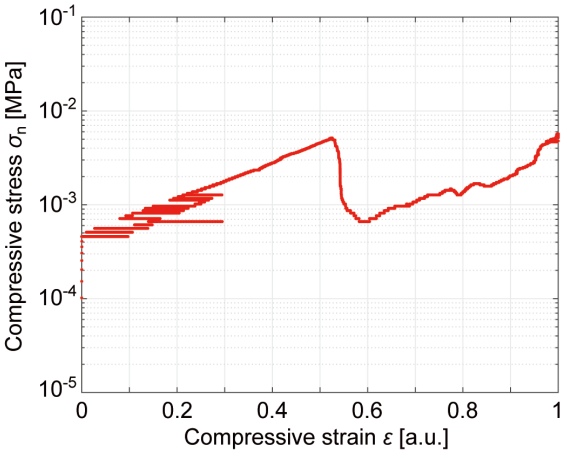

Sample 4

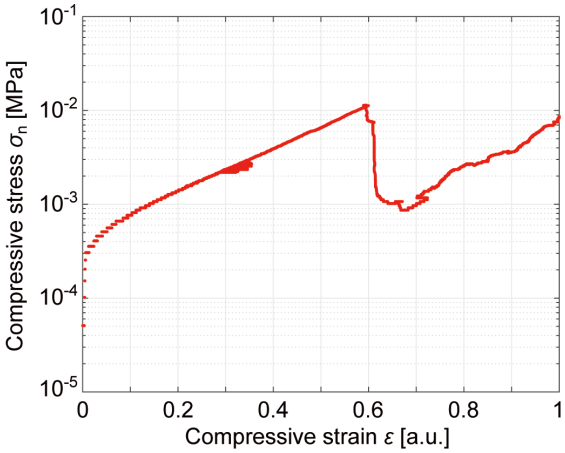

Sample 5

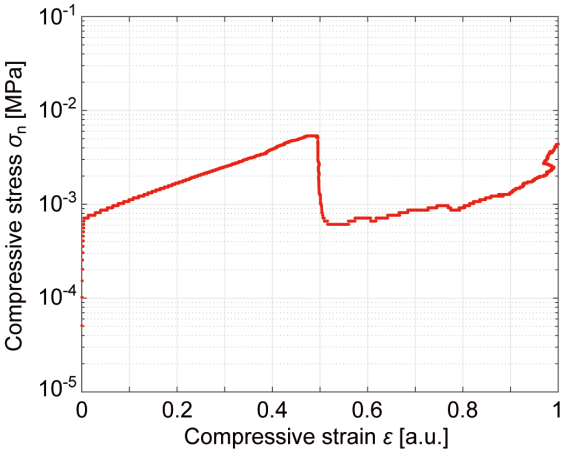

Supplementary Fig.14. Raw stress–strain data for cylindrical gelatin samples at 5 °C.